

Ultra-dense grid strategies for 3D GPR in Archaeology

Alexandre Novo, Henrique Lorenzo, Fernando I. Rial, Manuel Pereira, Mercedes Solla

EUET Forestal. University of Vigo

Campus A Xunqueira s/n. 36005-Pontevedra (Spain)

alexново@uvigo.es, hlorenzo@uvigo.es, firv@uvigo.es, airmanu@gmail.com, merchisolla@uvigo.es

Abstract - Understanding of GPR results by non-geophysicists has always been a long time challenge to overcome. However, the improvement of 3D imaging and processing software plus the application of different dense grid methodologies within the last few years have produced great results. So nowadays 3D GPR surveys are able not only to find but also obtain 3D reconstructions of buried objects. In this GPR investigation at convent of Santo Domingo (Lugo, Spain) a mudéjar sarcophagus is found where it was not expected to be attending to historical records. Moreover, images of its shape are obtained after applying a 3D GPR ultra-dense grid methodology and several 3D imaging techniques.

Keywords – GPR, 3D imaging, archaeology.

I. INTRODUCTION

The suitability of GPR in the location of man-made underground masonry (i.e., walls, galleries, crypts, etc.) is already well-known in the specialized bibliography [6], [8]. In this case, the target is quite different –a sarcophagus- and the main goal of the presented work is not only to find a sarcophagus but also define its shape by testing different ultra-dense grid methodologies as well as several 3D imaging techniques.

Such techniques have been successfully applied in GPR surveys along different archaeological sites such as: Roman buildings, Japanese burial mounds and other historical sites [1], [4], [5], [7] and [9]. These are commonly wide open areas with large targets that often have a well-known geometry. So usually these “pseudo 3D” GPR surveys are characterized by the use of mid-low frequency antennas with a space between profiles of half a meter which involves a vast interpolation among data. Such methodology is generally considered sufficient to obtain images with enough resolution to show the shape of those archaeological targets.

On the other hand, 3D GPR ultra-dense grid methodologies based on the Nyquist theorem are employed to obtain 3D and 4D imaging of the shallow subsurface [2]. The complexity of the targets (sand stratigraphy, fractures, tree roots, etc.) makes impossible to get 3D high resolution images by only applying image processing unless the grid spacing is reduced to a quarter of the wavelength in the host material.

As full-resolution 3D GPR imaging requires at least quarter wavelength grid spacing in all directions especially for a heterogeneous subsurface [3], several grids were designed by following this criteria and deducing the most suspected sites by real-time data interpretation as well as some rapid 3D data processing.

Not using laser devices for accurate positioning of the profiles was not seen as a problem in this case because of the special characteristics of the floor, the extremely care of the operators and the very small grid size in comparison with the target dimensions. However, the use of a more accurate navigation system would be necessary so as to prevent irregular distribution of GPR lines.

In addition, different software were applied and combined so as to obtain a large variety of displays and to find the most reliable 3D results. Easy 3D software of Malá Geoscience was used to build rough 3D cubes from raw data in order to rapidly visualize first results and then choose the right dataset for deeper processing methods.

A more advanced 3D imaging analysis was done within ReflexW v4.5.5 and GPR-SLICE v5.0 Software. After applying a basic signal processing flow (dewow and manual gain), several 3D imaging techniques such as: isosurface rendering and overlay analysis offered the best results. Animations, overlapped time-slices and isosurface renders have helped to discern the shape of the sarcophagus and to interpret the prospection data.

Moreover, these datasets were divided into others according to different profile spacing in order to find out the influence of GPR data decimation in the visualization of the different targets.

II. SURVEY SITE

Santo Domingo convent was the first convent of Lugo (Galicia) in the northwest of Spain (see Figure 1). A Dominican monk called Pedro López de Aguiar (1349-1390) become prior of the monastery, bishop of Lugo and confessor of the king of Castile, known as Pedro de Cruel. From historical records, it is known that he inherited a mudéjar sarcophagus to be buried inside of the convent. The shape of this sarcophagus is expected to be similar to another one exposed in the church (see Figure 2). According to the historians, the sarcophagus should be buried in the chapel of San Pedro Mártir which is the

smallest one and its wooden floor is not well preserved. However, GPR results denied that that site was the right one whereas proposed the Major chapel. It includes the actual pulpit where the masses are celebrated and its new floor is composed by marble. Both chapels are separated by a partition wall.

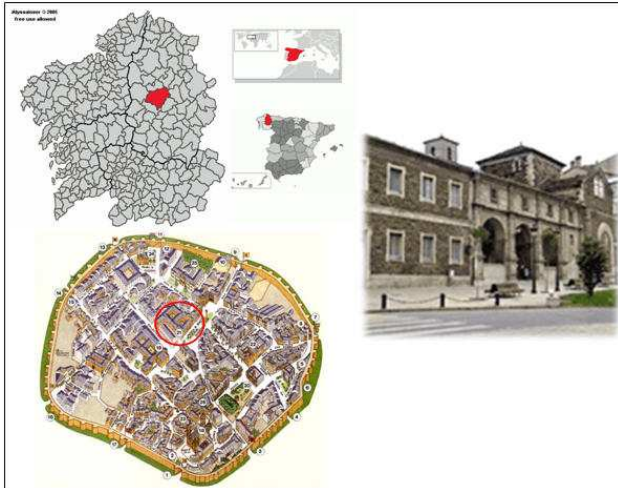


Figure 1. Location of the Santo Domingo convent in Lugo, Spain.

The small indoor areas allowed a meticulous work and a large number of parallel profiles very close to each other were recorded in X and Y directions. Despite the fact that the profile parallelism was facilitated by the alignments of the floor tiles, measurement tapes and strings were utilized to accurately design the grid.

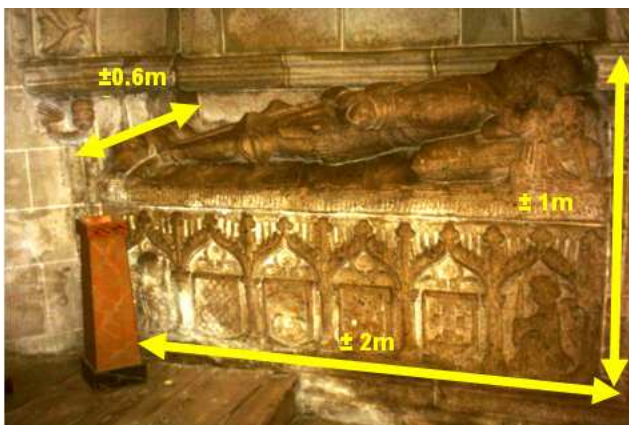


Figure 2. Expected dimensions of the sarcophagus.

III. ULTRA-DENSE GRID METHODOLOGY

3.1 Nyquist Theorem

According to the Nyquist condition or the Shannon sampling theorem, proper sampling or unaliased sampling data of each coordinate of the wavefield is achieved if:

$$\Delta x_m \leq V_{\min}/4f_{\max}$$

Where

x_m : midpoint coordinate

V_{\min} : minimum phase velocity of events

f_{\max} : maximum frequency

As $\lambda = V/f$, the Nyquist sample interval is one quarter of the wavelength in the host material.

$$\Delta x_m \leq \lambda/4$$

If the continuous wavefield is sampled according to the last equation then aliasing, temporal or spatial, does not occur. On the other hand, if the station spacing is greater than the Nyquist sampling interval, the data will not adequately define steeply dipping reflectors or diffraction tails. In areas of flat lying reflectors, this criterion can be compromised. The migration result depends on the sampling quality so theoretically, the best possible resolution can only be obtained with proper sampling of the data to be migrated. As an important conclusion, only proper or alias-free sampling of the data leads to a well-behaved migration operator response [10].

Very powerful interpolation techniques have been developed to compensate for undersampling. These techniques such as Krigging or Inverse Distance can interpolate “beyond Nyquist”, because additional information is provided. Whether such techniques should be relied upon to relax spatial sampling requirements is open to debate.

Table 1. Required grid spacing according to Nyquist theorem and in-line/cross-line settings used in the survey (velocity = 6 - 12 cm/ns)

Frequency	250	500
Grid spacing required ($\lambda/4$)	6-12 cm	3-6 cm
In-line spacing used	1 cm	1 cm
Cross-line spacing used	10 cm	5 cm

3.2 Survey Design

Malâ Ramac equipment composed by 250, 500 and 800 MHz shielded bistatic antennas with an odometer wheel was used in order to cover different depths and resolutions because of the uncertain situation of the sarcophagus.

First surveys were carried out in the chapel of San Pedro Mártir because of the recommendations of local historians. Some arbitrary profiles in X and Y directions with the 800 MHz antenna were done in order to test the capability of this antenna in terms of penetration depth.

After poor results trying with high frequency, two ultra-dense grids in both directions with the 250 MHz antenna were applied to survey the whole area with 57 profiles and 10 cm spacing. Real time interpretation and some rough 3D imaging results showed some shallow anomalies in the X direction but the resolution was insufficient.

Therefore, third step was the design of an ultra-dense grid of 43 profiles in the X direction separated 5 cm with the 500 MHz antenna. The image resolution of the shallower reflections improved. However, significant buried remains were not found in this chapel.

The other possibility that the historians had taken in consideration was the subsurface of the Major chapel. A 220 by 135 cm. grid composed by 28 profiles in perpendicular direction to the target were acquired in the most suspicious site of the Major chapel with a 500 MHz antenna which was selected as the most suitable frequency antenna for this survey.

Measurement tapes and strings were utilized to design every grid with extremely care by the three people involved in this project in order to overcome the lack of laser positioning sensors.

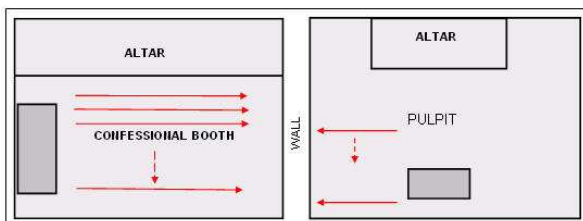


Figure 3. Sketch of San Pedro Mártir chapel (left) and Major chapel (right). Arrows indicate GPR profiles direction (500 MHz antenna).

IV. 3D IMAGING RESULTS

After applying a simple 2D filter flow, which consists in the subtraction of the DC drift and the application of manual gain on the data, some rough 3D cubes were created in order to visualize the first results and then choose the right dataset for deeper processing methods. Different 3D visualization techniques were applied to every dataset recorded.

4.1 San Pedro Mártir Chapel

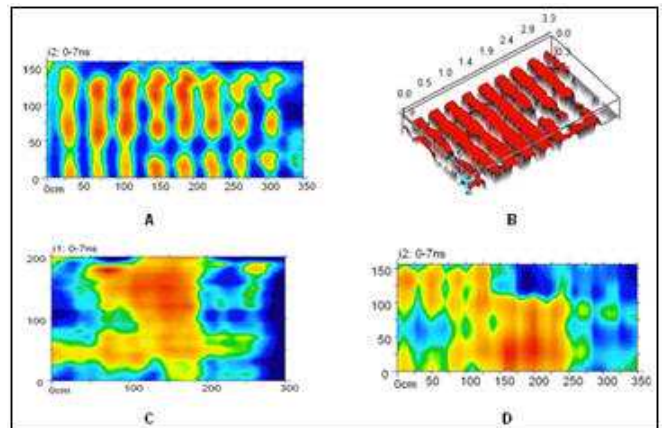


Figure 4. Time-slice at 7 ns (A) and isosurface render (B) with the 500 MHz antenna in X direction. Time-slices at 7 ns with the 250 MHz antenna in Y direction (C) and X direction (D).

Here, the crossbeams are clearly visible after 3D processing of data collected in X direction with the 500 MHz shielded antenna whereas they are almost invisible or at least individually indistinguishable by applying the same processing flow with data collected with the 250 MHz antenna in both directions.

Three decimated datasets extracted from the original 500 MHz dataset were processed in the same manner in order to compare the capability of detecting the crossbeams when the cross-line spacing increases (see Figure 5).

The linearity of the crossbeams permits to visualize them even with a cross-line spacing three times coarser than that given by the Nyquist criterion. From a value of 20 cm. the image quality decreases considerably.

Navigation errors during the acquisition due to a time-delay between the triggering system and the encoder of the odometer wheel are clearly visible in the time-slices presented below. An inappropriate pulling speed of the antenna plus an incorrect parameter setting could have been the reasons of this delay which has caused a random error in the data positions as shown in Figure 6.

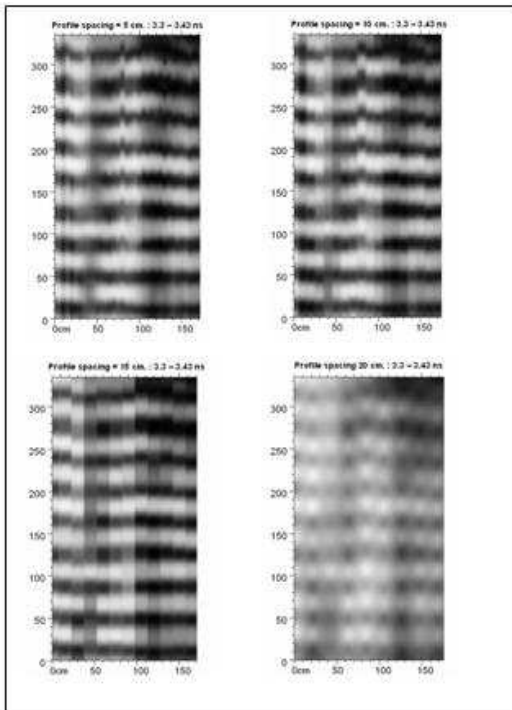


Figure 5. Time-slices (at 3 ns) of the 500MHz antenna survey in San Pedro Mártir chapel. Cross-line spacing from 5 cm (top left) to 20 cm (bottom right).

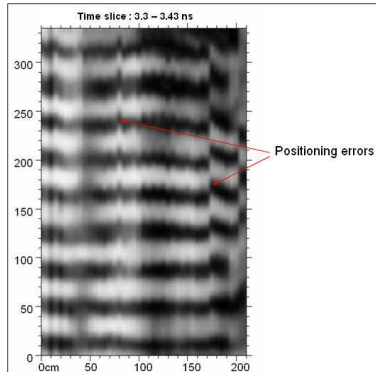


Figure 6. Time-slices from 5 cm. cross-line spacing show disturbances caused by (x,y) positioning errors

4.2 Major Chapel

As it is shown in Figure 7, decimation of the profile spacing from 5 cm to 20 cm does not affect much the visualization of the main target. The small size of the grid in comparison with the dimensions and regular shape of the target make possible that interpolation techniques can compensate for undersampling in this case.

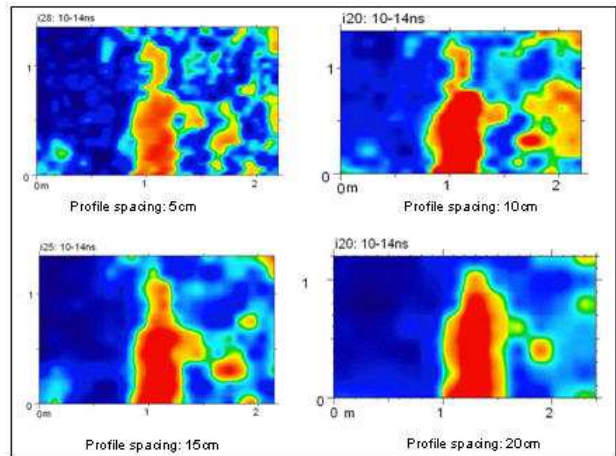


Figure 7. Comparison of unmigrated time-slices at 10-14 ns with different profile spacing.

Due to the special characteristics of this site in terms of dimensions, time slices of the unmigrated data look similar to those migrated in terms of interpretation. Also the background filter did not show any evident improvement in this particular dataset.

4.3 3D-Imaging Techniques

Overlay analysis technique allowed the linkage of structures buried at different depths. The relative strongest reflectors of the selected slices were summed and placed onto a single horizontal slice. In case the sarcophagus was inclined or even its relief in the upper part could cause anomalies at different levels in depth, overlay analysis was applied to overcome these hypothetical problems. However, the resulting information provided by this technique did not resolve new outstanding features.

Eventually, the extraction of a 3D volume which represents the target was possible by using the isosurface rendering technique. This technique displays surfaces of equal amplitude in the 3D volume. The threshold setting is a crucial decision. In this case, high threshold values shade our target because of stronger reflectors above it meanwhile lowering the threshold value, the target disappears completely. As the maximum values of amplitudes were placed in the first 10 ns, the shallowest data were eliminated in order to obtain a clearer isosurface render of the target (see Figure 8).

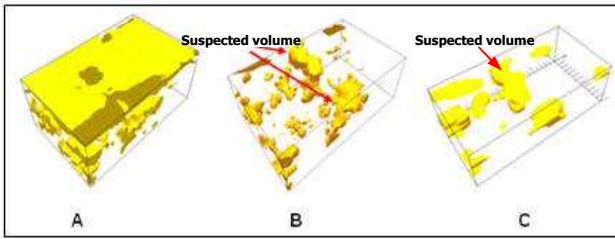


Figure 8. For A, B and C, same threshold value (70 %) and orientation. **A:** Whole data cube and 5cm profile spacing. **B:** Suspected volume after deleting the top 10 ns data from cube A. **C:** Suspected volume after decimating the profile spacing from 5cm (cube B) to 20cm.

V. CONCLUSIONS

Intuitive comprehension of geophysical data by archaeologists or historians can be very useful as well as cost-saving for planning most archaeological excavations and this purpose is achieved by displaying the GPR data in this way.

Comparison among the present work and previous searches of other man-made masonry structures such as voids or crypts shows that the application of 3D imaging techniques can be really worth it.

The visualization of the sarcophagus is quite similar with a profile spacing of 5 cm, 15 cm or even 20 cm. These results indicate that, in this particular case -searching for a big target in a small area-, the extra effort to acquire ultra-dense grids have not provided more archaeological information. Nevertheless, the application of ultra-dense grid strategies and a finer 3D data processing allowed detecting navigation errors during the GPR acquisition due to a time-delay between the triggering system and the encoder of the odometer wheel.

As well, animations and renders of the decimated datasets have also shown similar results. Therefore, the loss of information between GPR lines was not crucial to define the sarcophagus. However, the same decimation of the data acquired over the crossbeams in San Pedro Mártir chapel has shown some changes in terms of image sharpness.

Eventually, ultra-dense grid strategies have managed to reconstruct the different targets three-dimensionally as well as find out how results are affected by data decimation and inaccurate positioning of traces.

ACKNOWLEDGMENTS

This research work has been carried out under financial support of Xunta de Galicia (PGIDIT06CST101PR, 2006-09) and partial support of the University of Vigo (Research Grants Program 2007).

REFERENCES

- [1] Goodman, D, J. Steinberg, B. Damiata, Y. Nishimura, K. Schneider, H. Hiromichi, N. Higashi., GPR Overlay Analysis for Archaeological Prospection. Proceedings of the 11th International Conference on Ground Penetrating Radar 2006, Columbus, Ohio, USA.
- [2] Grasmueck, M. and D.A. Viggiano. 3D/4D GPR Toolbox and Data Acquisition Strategy for High-Resolution Imaging of Field Sites. Eleventh International Conference on Ground Penetrating Radar, June 19-22, 2006, Columbus, Ohio, USA.
- [3] Grasmueck, M., R. Weger, and H. Horstmeyer. 2004. Full-resolution 3D Imaging for Geoscience and Archeology. Tenth International Conference on Ground Penetrating Radar, 21-24 June, 2004, Delft, The Netherlands.
- [4] Leckebusch, J. 2003. Ground-Penetrating Radar: A Modern Three-dimensional Prospection Method. *Archaeological Prospection*, 10, 213-240.
- [5] Leucci G and S. Negri. 2005. Use of ground penetrating radar to map subsurface archaeological features in an urban area. *Journal of Archaeological Science*, 33, 502-512.
- [6] Lorenzo, H., M.C. Hernández and V.Cuellar. 2002. Selected radar images of man-made underground galleries, *Archaeological Prospection*, vol. 9, pp 1-7.
- [7] Lualdi, M., L. Zanzi and G. Sosio. 2006. A 3D GPR Survey Methodology for Archaeological Applications. Eleventh International Conference on Ground Penetrating Radar, June 19-22, 2006, Columbus, Ohio, USA.
- [8] Martinaud, M., M. Frappa and R. Chapoulie. 2004. GPR signals for the understanding of the shape and filling of man-made underground masonry. Tenth International Conference on Ground Penetrating Radar, 21-24 June, 2004, Delft, The Netherlands.
- [9] Nuzzo, L., G. Leucci, S. Negri, M.T. Carrozzo, and T. Quarta. 2002. Application of 3D visualization techniques in the analysis of GPR data for archaeology. *Annals of Geophysics*, vol. 45, N. 2.
- [10] Vermeer G.J.O., *3D Seismic survey design: Geophysical Reference Series 12*, SEG. (2002).